Structural and Functional Abnormalities of the Primary Somatosensory Cortex in Diabetic Peripheral Neuropathy: A Multimodal MRI Study

Dinesh Selvarajah,[1] Iain D. Wilkinson,[2] Fang Fang,[3] Adithya Sankar,[2] Jennifer Davies,[2] Elaine Boland,[2] Joseph Harding,[1] Ganesh Rao,[3] Rajiv Gandhi,[4] Irene Tracey,[5] and Solomon Tesfaye[4]

Diabetes 2019;68:796–806 | https://doi.org/10.2337/db18-0509

Downloaded from http://diabetesjournals.org/diabetes/article-pdf/68/4/796/523542/db180509.pdf by guest on 27 August 2022

COMPLICATIONS

Diabetic distal symmetrical peripheral polyneuropathy (DSP) results in decreased somatosensory cortical gray matter volume, indicating that the disease process may produce morphological changes in the brains of those affected. However, no study has examined whether changes in brain volume alter the functional organization of the somatosensory cortex and how this relates to the various painful DSP clinical phenotypes. In this case-controlled, multimodal brain MRI study of 44 carefully phenotyped subjects, we found significant anatomical and functional changes in the somatosensory cortex. Subjects with painful DSP insensate have the lowest somatosensory cortical thickness, with expansion of the area representing pain in the lower limb to include face and lip regions. Furthermore, there was a significant relationship between anatomical and functional changes within the somatosensory cortex and severity of the peripheral neuropathy. These data suggest a dynamic plasticity of the brain in DSP driven by the neuropathic process. It demonstrates, for the first time in our knowledge, a pathophysiological relationship between a clinically painful DSP phenotype and alterations in the somatosensory cortex.

Distal symmetrical peripheral polyneuropathy (DSP) develops in up to 50% of patients with diabetes (1). Most patients develop a painless neuropathy that increases the risk of foot ulceration and subsequent amputation. A significant proportion of patients also develop a chronic painful condition that can result in considerable disability and suffering (2,3). Detailed sensory phenotyping has shown distinct sensory profiles of patients with painful compared with painless DSP (4). Moreover, the sensory profiles of patients with painful DSP were not homogeneous, with a significant proportion of patients demonstrating positive sensory signs, such as dynamic mechanical allodynia (4). No clear pathophysiological explanation exists for this spectrum of neuropathic phenotypes in DSP. Much of the research focus has been on the peripheral nervous system only, with potential central nervous system (CNS) involvement largely overlooked. Although some evidence for CNS involvement has emerged recently (5–7), further research of the extent of this involvement may be crucial for a greater understanding of the pathologic mechanisms of DSP, now made possible with advances in noninvasive MRI (8).

Structural and functional cortical plasticity is a fundamental property of the human CNS that enables adjustment to nerve injury (9,10). However, it can have maladaptive consequences, possibly resulting in chronic pain (11–13). We have previously demonstrated a clear reduction in both spinal cord cross-sectional area (14,15) and primary somatosensory cortex (S1) (16) gray matter volume in DSP. Studies in other pain conditions also have reported dynamic structural and functional plasticity that have profound effects on the brain in patients with neuropathic pain (17–19). Collectively, these studies led us to hypothesize that both structural and

[1]Department of Human Metabolism, University of Sheffield, Sheffield, U.K.
[2]Academic Unit of Radiology, University of Sheffield, Sheffield, U.K.
[3]Department of Neurophysiology, Sheffield Teaching Hospitals NHS Foundation Trust, Sheffield, U.K.
[4]Diabetes Research Department, Sheffield Teaching Hospitals NHS Foundation Trust, Sheffield, U.K.
[5]Oxford Centre for Functional MRI of the Brain (FMRIB), Oxford University, Oxford, U.K.

Corresponding author: Dinesh Selvarajah, d.selvarajah@sheffield.ac.uk

Received 13 June 2018 and accepted 13 December 2018

This article contains Supplementary Data online at http://diabetes.diabetesjournals.org/lookup/suppl/doi:10.2337/db18-0509/-/DC1.

© 2019 by the American Diabetes Association. Readers may use this article as long as the work is properly cited, the use is educational and not for profit, and the work is not altered. More information is available at http://www.diabetesjournals.org/content/license.

functional brain plasticity underly the various clinical phenotypes of DSP. Hence, the principal aim of this study was to use combined, structural, and functional MRI (fMRI) to examine the organization of the S1 in DSP. To our knowledge, no study has examined this previously in DSP. If DSP is associated with cortical plasticity, then these changes may ultimately determine the clinical phenotype.

RESEARCH DESIGN AND METHODS

The study included 44 right-handed subjects (35 with type 1 diabetes and 9 healthy volunteers [HVs]). Inclusion criteria were type 1 diabetes for >5 years, right-handedness, age between 18 and 65 years, stable glycemic control (HbA_{1c} <11% [97 mmol/mol]), and willingness to discontinue neuropathic pain medications before MRI scan. Exclusion criteria were clinical evidence of disease in the CNS (e.g., cerebrovascular disease), nondiabetic neuropathies, history of alcohol consumption of >20 units/week (1 unit is equivalent to 1 glass of wine or 1 measure of spirits), diabetic neuropathies other than DSP (e.g., mononeuropathies, proximal motor neuropathies), epilepsy, recurrent severe hypoglycemia, hypoglycemic unawareness, psychiatric conditions, or claustrophobia or other factors that preclude MRI. We also recruited age- and sex-matched, right-handed, HVs without diabetes. All HVs were free of chronic pain conditions and were not using analgesic medications or alternative therapies for pain. Written informed consent was obtained before participation in the study, which had prior approval by the Sheffield local research ethics committee (reference number 08/H1308/276).

Sensory Phenotyping

All subjects underwent detailed clinical and neurophysiological assessments. The outcome of a detailed upper- and lower-limb neurological examination was graded using the Neuropathy Impairment Score questionnaire (20). The following neurophysiological assessments were then performed: *1*) vibration and warmth thermal pain detection thresholds acquired from the dorsal aspect of the right foot using the CASE IV system (WR Medical Electronics, Maplewood, MN) using standard techniques (21,22), *2*) cardiac autonomic function tests performed with a computer-assisted technique according to O'Brien's protocol (23), and *3*) nerve conduction studies performed at a stable skin temperature of 31°C and a room temperature of 24°C using a Medelec Synergy electrophysiological system (Oxford Instruments, Oxford, U.K.). The following nerve attributes were measured: *1*) sural sensory nerve action potentials and conduction velocities and *2*) common peroneal and tibial motor nerve distal latency, compound muscle action potential, and conduction velocity. An overall neuropathy composite score (NCS) derived from transformed percentile points of abnormalities in nerve conduction studies, vibration detection thresholds, and heart rate variability with deep breathing was calculated in accordance with criteria proposed by Dyck et al. (24). On the basis of the Toronto consensus statement (23), all subjects with DSP had confirmed neuropathy with at least two abnormalities on neurophysiological assessments.

Painful DSP Sensate Versus Insensate

Painful DSP was defined according to International Association for the Study of Pain definition of neuropathic pain (25) and scored using the Neuropathy Total Symptom Score-6 (NTSS-6) questionnaire (26). NTSS-6 evaluates the frequency and intensity of neuropathic sensory symptoms frequently reported in DSP (i.e., numbness and/or insensitivity, prickling and/or tingling sensation, burning sensation, aching pain and/or tightness; sharp, shooting, lancinating pain; allodynia and/or hyperalgesia). Only subjects with painful DSP with distal symmetrical painful neuropathic symptoms involving the feet and legs present for at least 6 months were included.

On the basis of clinical and neurophysiological assessments subjects with painful DSP were divided into two groups: painful DSP insensate (n = 8), wherein subjects are characterized by lower-limb sensory loss dominated by small- and large-fiber clinical and neurophysiological abnormalities, likely representing the deafferentation or painful hypoesthesia phenotype (27), and painful DSP sensate (n = 9), wherein subjects have with relatively preserved small- and/or large-fiber function in combination with thermal (heat) hyperalgesia and low-intensity dynamic mechanical allodynia, likely representing the sensory gain phenotype or irritable nociceptor subgroup described by others (24). The remaining subjects with diabetes were divided into two control groups (28): no DSP (n = 9), wherein asymptomatic subjects have normal clinical and neurophysiological assessments, and painless DSP (n = 9), wherein subjects have painless neuropathy with abnormal clinical assessment and at least two abnormalities on neurophysiological assessment.

Psychophysics

Before MRI, we performed a pain calibration procedure using methods described in previous work (29) (Supplementary Data). For each subject, we determined the temperature required to obtain a pain score of at least 7 using a numeric rating scale (NRS) (0 = no pain, 10 = worse pain imaginable). A maximum temperature of 47.9°C was used to prevent scalding.

MRI Acquisition and fMRI Task Design

We used a 3.0 T scanner (Achieva 3T; Philips Medical Systems, Holland, the Netherlands) to scan all subjects. Anatomical data were acquired using a T1-weighted magnetization prepared rapid acquisition gradient echo sequence with the following parameters: repetition time 7.2 ms, echo time 3.2 ms, flip angle 8°, and voxel size 0.9 mm^3, yielding isotropic spatial resolution. Functional data on the basis of the blood oxygenation level–dependent

Downloaded from http://diabetesjournals.org/diabetes/article-pdf/68/4/796/523542/db180509.pdf by guest on 27 August 2022

(BOLD) signal were acquired using a single-shot gradient echo-planar T2*-weighted pulse sequence, with the following parameters: repetition time 3,000 ms, echo time 35 ms, and in-plane pixel dimensions 1.8 × 1.8 mm. Contiguous transaxial slices with slice thickness of 4 mm were oriented in the oblique axial plane parallel to the anterior-posterior commissure bisection, covering the whole cortex, with partial coverage of the cerebellum. Two hundred three temporal dynamics were acquired per boxcar function run. Throughout scanning, we also continuously monitored heart rate (electrocardiogram and peripheral pulse) and respiration through the built-in scanner monitoring/triggering device (Philips Medical Systems).

After calibration and training, subjects were positioned in the scanner, and an MRI-compatible heat probe was place on the dorsum of the right foot or anterior aspect of the thigh. Subjects were randomized to begin stimulation of either the foot or the thigh. During each period, fMRI images were acquired over seven functional runs. A classic block design was used consisting of baseline and stimulus, alternating seven times. Each functional run comprised an alternating 30-s period of tonic heat stimulation followed by rest. The intensity of painful heat stimulation applied to the foot and thigh was calibrated for each subject. The slope of thermal stimulus applied was 5°C/s. Thermal stimulus was delivered using a Peltier-driven thermotest device with an fMRI-compatible thermode (probe size 3 × 3 cm, PATHWAY Model CHEPS neurosensory analyzer; Medoc, Ramat Yishai, Israel). The duration of rest periods was pseudorandomized to 50, 55, and 60 s to minimize the anticipation of the next stimulation period (Fig. 1 and Supplementary Data). Subjects were instructed to keep still during the scanning, which was verified visually. At the end of the scan, subjects once again were asked to rate the level of heat pain in the foot and thigh experienced during the fMRI. We also asked subjects to rate the unpleasantness of the experience when heat pain was applied to the foot and thigh (separately) using an NRS (0 = not unpleasant/tolerable, 10 = extremely unpleasant/intolerable).

MRI Analyses

Cortical Thickness

Cortical reconstruction and volumetric segmentation were performed with FreeSurfer software (http://surfer.nmr.mgh.harvard.edu). This processing includes motion correction and averaging (30) of volumetric T1-weighted images, removal of nonbrain tissue using a hybrid watershed/surface deformation procedure (31), affine registration to the Talairach atlas (32,33), intensity normalization, tessellation of the gray matter-white matter boundary, automated topology correction (34,35), and surface deformation following intensity gradients to optimally place the gray/white and gray/cerebrospinal fluid borders at the location where the greatest shift in intensity defines the transition to the other tissue class (36,37). Surface-based maps are created from the intensity and continuity information from the entire three-dimensional MR volume in segmentation and deformation procedures to produce representations of cortical thickness calculated as the closest distance from the gray/white boundary to the gray/cerebrospinal fluid boundary at each vertex on the tessellated surface (34). Cortical thickness (in mm, sensorimotor regions S1 and precentral cortex) and deep brain nuclei volumes (in mm^3, thalamus, caudate, and insula) were measured. Results of cortical thickness analyses are presented in Table 3 and Fig. 2. Significant differences in regional cortical thickness and deep brain nuclei volumes among study cohorts were examined using ANOVA. In addition, S1 cortical thickness

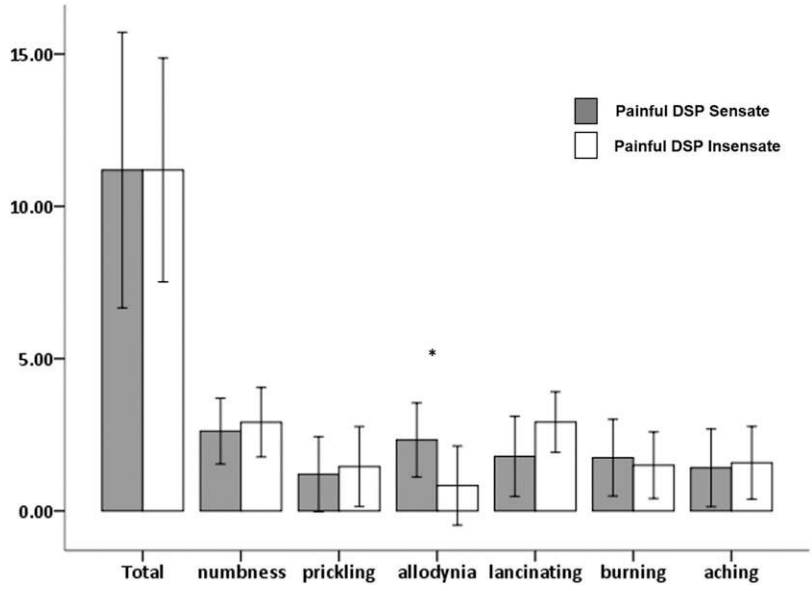

Figure 1—Sensory descriptors. Means and 95% CIs of the six pain descriptors and total score from the NTSS-6 by subjects with painful DSP sensate and insensate. *$P < 0.05$.

Downloaded from http://diabetesjournals.org/diabetes/article-pdf/68/4/796/523542/db180509.pdf by guest on 27 August 2022

that significantly correlated to the degree of neuropathy severity (NCS), and pain scores (NTSS-6 and evoked pain) were determined in subjects with painful DSP (sensate and insensate) using Pearson correlation for normally distributed data and Spearman rank correlation for nonnormally distributed data. This analysis was used to examine the association between volume changes in the S1 and markers of neuropathy severity.

fMRI Analysis

MRI data acquisition, preprocessing (FNIRT), and analyses followed standard procedures (Supplementary Data). Functional imaging data were processed using the Oxford Centre for Functional MRI of the Brain (FMRIB) expert analysis tool FEAT version 5.98 (www.fmrib.ox.ac.uk/fsl) (38). To allow us to focus specifically on topographical shifts in body part representation, we conducted two different analyses.

Cortical Distance Analysis of Peak Activation. First, we examined differences in the Euclidean distances (EDs) of peak activation within the contralateral S1. A region of interest (ROI) comprising the contralateral S1 was used to restrict the fMRI analysis to the gray matter of the S1 for each subject. The maximally activated voxel within this ROI during each tonic heat stimulation paradigm was determined. The spatial position of this voxel was located for each subject by measuring the ED between it and a standard anatomical point (the point at which the central sulcus meets the longitudinal fissure at the dorsal aspect of the brain). This procedure has been described in detail previously (13). The ED between the anatomical marker and the maximally activated voxel in the S1 ROI was computed for the anterior-posterior, medial-lateral, and superior-inferior coordinates. The ED between two points was calculated using the Pythagorean theorem and provided an absolute value independently of direction (12). An ANOVA was used to determine the significant differences in the ED of peak S1 activation between study cohorts. However, the ED method only examines the differences in the location of peak activation during thermal nociceptive stimulation between cohorts; it does not examine the full extent of neuronal activation.

Analysis of the Extent of S1 Receptive Field Activation. Next, to examine the group differences in the extent of S1 activation, we estimated activity maps for each condition (foot and thigh stimulation) within each subject by applying a voxel-based general linear model, as implemented in FEAT. For each subject, a set of regressors was constructed for conditions of interest (heat stimulation of the foot and thigh) using the block design paradigm convolved with a γ-function, and its temporal derivative was used to model the activation time course. The parameter estimates (regression slopes) for each condition thus provided an estimate at each voxel of the activation intensity for that condition. The second-level analysis (i.e., group analysis) was performed to identify condition-specific patterns of activation for each group (i.e., HV, no DSP, painless DSP, painful DSP sensate, painful DSP insensate). This whole-brain group-level analysis was carried out using FMRIB's local analysis of mixed effects (39). The main condition contrasts were defined using painful DSP insensate as the main comparator group versus *1*) HV, *2*) no DSP, *3*) painless DSP, and *4*) painful DSP sensate. Z (Gaussianized T/F) statistic images were thresholded using clusters determined by $Z > 2$, and a family-wise error–corrected cluster significance threshold of $P < 0.05$ was applied to the suprathreshold clusters to correct for multiple comparisons. For presentation purposes, the activation maps were smoothed using a full-width at half maximum of 4 mm and thresholded at $Z > 1.5$. A group-level analysis was performed using FMRIB's local analysis of mixed effects, with painful DSP insensate as the main comparator group. Using this analysis, we compared the pattern of neuronal activation in subjects with painful DSP insensate with the other study cohorts. We asked which brain regions are more active during nociceptive warm thermal stimulation in subjects with painful DSP insensate compared with the other cohorts and vice versa. The resulting maps were visually inspected to verify that the clusters of activation were located along the S1 strip. For each comparison, we identified voxels within the S1 that displayed significant increases in signal intensity. In each subject, we determined the percent change during nociceptive warm thermal stimulation (relative to baseline rest periods) in signal intensity over time centered around the maximally activated voxel and the significant differences between groups assessed (Mann-Whitney U test $P < 0.05$). In addition, Z scores of S1 signal intensity that were significantly correlated to severity of neuropathy (NCS), pain scores (NTSS-6 and evoked pain scores), and S1 cortical thickness were determined using Pearson correlation for normally distributed data and Spearman rank correlation for nonnormally distributed data. This analysis was performed to examine the association between the functional reorganization of the S1 and S1 cortical volume changes and clinical markers of neuropathy severity. The Z score was chosen because it is assumed to be more appropriate than the magnitude of difference in that it also considers the variance in the signal.

Statistical Analyses

Statistical analysis was carried out with SPSS version 21 software (IBM Corporation). Group differences on demographic characteristics and psychophysical experiments were compared using ANOVA. Subsequent subgroup comparisons were performed using a post hoc analysis.

RESULTS

Overall, subjects with DSP were older ($F[4,39] = 0.36$, ANOVA $P = 0.83$) than subjects with no DSP. To minimize the potential effect of age on study outcome measures, we recruited an older cohort of HVs. No significant difference was found in duration of diabetes between the diabetes groups ($F[3,31] = 0.53$, ANOVA $P = 0.98$) (Table 1). There were no significant differences in post hoc analyses of

Downloaded from http://diabetesjournals.org/diabetes/article-pdf/68/4/796/523542/db180509.pdf by guest on 27 August 2022

Table 1—Demographic characteristics of each study cohort

	HV	No DSP	Painless DSP	Painful DSP sensate	Painful DSP insensate	*P* value
n	9	9	9	9	8	
Age (years)	51.5 (7.9)	45.9 (10.1)	46.3 (12.1)	48.4 (12.0)	44.5 (12.1)	0.83
Sex, male (*n*)	1	6	7	5	6	**0.03**
Diabetes duration (years)	NA	22.8 (14.9)	21.4 (8.1)	23.4 (10.2)	23.2 (12.6)	0.98
Pain duration (years)	NA	NA	NA	6.8 (6.3)	7.8 (7.3)	0.76
HbA_{1c} (mmol/mol)	NA	72.8 (17.4)	68.0 (7.7)	72.8 (13.9)	87.7 (28.1)	0.30
HbA_{1c} (%)	NA	8.8	8.4	8.8	10.2	
NTSS-6 score	NA	NA	NA	11.3 (5.1)	11.2 (4.4)	0.96
Vibration JND	NA	14.7 (2.2)	19.3 (4.6)	21.4 (3.9)	24.3 (1.7)	**0.002**
NCS	NA	1.4 (1.8)	10.6 (7.1)	9.0 (5.3)	19.1 (0.83)	**<0.001**
Retinopathy status (*n*)	NA					**0.03**
No DR		2	3	2	2	
Mild nonproliferative DR		7	3	4	0	
Moderate/severe nonproliferative DR		0	3	3	6	

Data are mean (SD) unless otherwise indicated. ANOVA was used to determine the *P* value. Boldface type indicates significance at $P < 0.05$. DR, diabetic retinopathy; JND, just noticeable difference; NA, not applicable.

group mean for age or duration of diabetes, and there was no significant difference in mean HbA_{1c} ($F[3,31] = 1.65$, ANOVA $P = 0.20$). As expected, a χ^2 test for independence indicated a significant association between neuropathy and retinopathy status ($\chi^2[6,35] = 13.8$, $P = 0.03$).

Sensory Profiling

All subjects with painful DSP had a distal symmetrical peripheral neuropathy that affected the feet and legs and was sparing of the thigh. Pain duration ($t[15] = 0.32$, $P = 0.76$) and intensity ($t[15] = 0.14$, $P = 0.89$) was comparable between the two painful DSP groups (Table 1). Using the NTSS-6 to assess pain descriptors, it was found that subjects with painful DSP reported typical neuropathic symptoms (Fig. 1). Those with painful DSP sensate, however, reported significantly higher mean scores for allodynia than those with painful DSP insensate (2.48 [1.4] vs. 0.83 [1.5], $t[15] = 2.27$, $P = 0.04$).

Psychophysics

No significant difference in temperature was applied to the foot ($F[4,39] = 1.3$, $P = 0.29$) (Table 2 includes post hoc analyses). Unsurprisingly, subjects with painless DSP and painful DSP insensate had the lowest NRS pain scores ($F[4,39] = 12.4$, ANOVA $P < 0.001$) and unpleasantness scores ($F[4,39] = 2.92$, ANOVA $P = 0.03$). Upon thigh stimulation, no significant difference was found in temperature ($F[4,39] = 1.03$, ANOVA $P = 0.40$), NRS pain ($F[4,39] = 0.59$, ANOVA $P = 0.67$), or unpleasantness ($F[4,39] = 0.24$, ANOVA $P = 0.92$) scores.

Cortical Thickness

Subjects with painful DSP insensate had significantly lower mean bilateral S1 (3.60 [0.1] mm, $F[4,39] = 5.78$, ANOVA $P = 0.001$) cortical thickness compared with other study cohorts (HV 4.04 [0.1] mm, no DSP 3.85 [0.2] mm,

Table 2—Results of psychophysical experiments conducted before MRI

	HV	No DSP	Painless DSP	Painful DSP sensate	Painful DSP insensate	*P* value
Foot						
Temperature	45.7 (1.1)	46.2 (1.3)	47.1 (1.0)	46.5 (1.1)	46.1 (1.7)	0.29
Pain score	8.1 (0.8)	8.1 (0.4)	5.4 (3.5)	7.4 (1.6)	1.6 (3.1)	**<0.001**
Unpleasantness score	7.2 (1.6)	7.1 (1.3)	5.6 (3.4)	5.5 (2.1)	3.4 (3.3)	**0.03**
Thigh						
Temperature	45.7 (1.4)	45.5 (1.2)	45.3 (1.6)	46.5 (0.7)	45.8 (1.4)	0.40
Pain score	7.5 (0.8)	7.7 (0.8)	7.9 (0.9)	7.1 (1.4)	7.5 (1.9)	0.59
Unpleasantness score	6.2 (2.3)	6.6 (1.4)	6.0 (2.8)	6.1 (1.8)	6.2 (2.3)	0.92

Data are mean (SD). Boldface type indicates significance at $P < 0.05$. Noxious thermal heat stimulation was applied to the right foot (neuropathic site) and thigh (nonneuropathic control site). Mean temperature required to achieve a pain score (0 = no pain, 10 = worst pain) of at least 7 was recorded. Subjects also were asked to rate unpleasantness (0 = not unpleasant, 10 = most unpleasant). Sequence of thermal stimulus application to foot and thigh was randomized across subjects. Post hoc analysis for foot pain score: painful DSP insensate vs. HV ($P < 0.001$), no DSP ($P < 0.001$), and painful DSP sensate ($P < 0.001$); painless DSP vs. HV ($P = 0.02$), no DSP ($P = 0.02$), and painful DSP sensate ($P = 0.06$); and painful DSP insensate vs. painless DSP ($P = 0.002$). Post hoc analysis for foot unpleasantness score: painful DSP insensate vs. HV ($P = 0.005$) and no DSP ($P = 0.006$).

Downloaded from http://diabetesjournals.org/diabetes/article-pdf/68/4/796/523542/db180509.pdf by guest on 27 August 2022

painless DSP 3.82 [0.2] mm, painful DSP sensate 3.88 [0.2] mm) (Table 3 [includes post hoc analyses] and Fig. 2). Unilateral evaluation showed significant differences in both left- and right-side S1 cortical thickness (F[4,39] = 5.30 [ANOVA P = 0.002] and 6.46 [ANOVA $P < 0.001$], respectively). On average, somatosensory cortical thickness was 12.2% lower in subjects with painful DSP insensate than in HVs. We also examined other pain, sensory, and motor processing areas, and the only other significant difference was in the precentral gyrus thickness (painful DSP insensate 4.43 [0.2] mm vs. HV 4.73 [0.2] mm, no DSP 4.74 [0.3] mm, painless DSP 4.63 [0.2] mm, painful DSP sensate 4.77 [0.2] mm; F[4,39] = 4.98; ANOVA P = 0.009). No significant difference emerged between painful DSP and other study cohorts in bilateral measures for caudate volume (F[4,39] = 0.92, ANOVA $P > 0.4$), and differences fell short of significance for thalamic volume (F[4,39] = 1.83, ANOVA P = 0.14) and insula cortical thickness (F[4,39] = 1.90, ANOVA P = 0.13). Unilateral evaluation showed no significant differences in either left- or right-sided caudate and a trend-level difference in left thalamus (F[4,39] = 2.17, ANOVA P = 0.09). For subjects with painful DSP (sensate and insensate), a moderate and significant correlation was found between foot-evoked pain scores and S1 cortical thickness but not for the precentral gyrus thickness (Fig. 2). Evoked foot pain scores, a measure of small c-fiber function and foot sensitivity, correlated with left-side (r = 0.44, P = 0.004) and right-side (r = 0.47, P = 0.002) S1 cortical thickness (Fig. 2*C*). Furthermore, there was a significant negative correlation between NCS and S1 cortical thickness (r = −0.60, P = 0.01) (Fig. 2*D*). No significant correlations were found between thigh-evoked pain scores and measures of cortical thickness. For subjects with painful DSP (sensate and insensate), there was no significant correlation between reported pain scores (NTSS-6) and measures of cortical thickness or volumes of deep gray matter nuclei. There was no significant difference in peripheral gray matter (F[4,39] = 1.2, ANOVA P = 0.32), total gray matter (F[4,39] = 0.85, ANOVA P = 0.50), and whole-brain (F[4,39] = 2.1, ANOVA P = 0.11) volumes among study groups.

fMRI

Because subjects with painful DSP insensate had the greatest reduction in S1 cortical thickness, we reasoned that there will be accompanying functional changes in the topographical organization of the S1. Statistical parametric maps showing brain areas significantly activated in response to stimulation are shown in Supplementary Fig. 3. In all groups, tonic heat stimulation of the right foot (Supplementary Fig. 3*A*) resulted in increased BOLD response in the left-side S1, thalamus, insula, and anterior cingulate gyrus consistent with the well-described representation of pain. Similar areas of increased BOLD response were seen with thigh stimulation (Supplementary Fig. 3*B*). In all subjects, tonic heat stimulation of the foot and thigh resulted in a lateral-to-medial pattern of activation within the contralateral S1, consistent with the sensory homunculus. The precise locations of S1 activations were similar in all four groups. The ED of peak activation within the left-side S1 was not significantly different across study groups for both foot (F[4,39] = 0.64, ANOVA P = 0.63) (Supplementary Fig. 2) and thigh (F[4,39] = 0.39, ANOVA P = 0.85) stimulation.

There were, however, significant differences in BOLD response in subjects with painful DSP insensate compared with the other study cohorts during both foot (Fig. 3) and thigh (Fig. 4) stimulation. That is, subjects with painful DSP insensate displayed significant S1 functional reorganization in which there was an expansion of the area representing pain in the lower limb to include regions representing the face and lips. Finally, there was

Table 3—Brain volumes, bilateral regional cortical thicknesses, and deep brain nuclei volumes

	HV	No DSP	Painless DSP	Painful DSP sensate	Painful DSP insensate	P value
Brain volume, mL						
Peripheral gray	626.7 (27.2)	622.6 (24.6)	604.9 (23.8)	606.8 (52.4)	591.6 (25.0)	0.32
Gray matter	792.9 (30.9)	788.7 (31.8)	767.9 (29.0)	763.6 (62.5)	777.5 (43.5)	0.50
White matter	729.8 (41.4)	721.0 (43.9)	709.8 (27.6)	694.5 (26.7)	751.3 (12.9)	**0.04**
Whole brain	1,522.7 (59.1)	1,509.6 (64.7)	1,477.7 (27.1)	1,458.0 (83.4)	1,528.9 (46.0)	0.11
Cortical thickness, mm						
Postcentral	4.04 (0.1)	3.85 (0.2)	3.82 (0.2)	3.88 (0.2)	3.60 (0.1)	**0.001**
Precentral	4.73 (0.2)	4.74 (0.3)	4.63 (0.2)	4.77 (0.2)	4.43 (0.2)	**0.009**
Deep brain nuclei volume, cm^3						
Thalamus	6.55 (0.5)	7.39 (0.8)	6.91 (0.4)	6.66 (0.9)	6.71 (0.8)	0.14
Caudate	3.40 (0.5)	3.64 (0.5)	3.67 (0.4)	3.41 (0.5)	3.68 (0.3)	0.46
Insula	5.81 (0.3)	5.89 (0.2)	5.90 (0.3)	5.71 (0.4)	5.56 (0.2)	0.13

Data are mean (SD). Boldface type indicates significance at $P < 0.05$. Post hoc analysis: white matter volume: painful DSP insensate vs. painless DSP (P = 0.03), painful DSP insensate vs. painful DSP sensate (P = 0.004), and HV vs. painful DSP sensate (P = 0.04); postcentral gyrus thickness: painful DSP insensate vs. HV ($P < 0.001$), no DSP (P = 0.008), painless DSP (P = 0.02), and painful DSP sensate (P = 0.003); precentral gyrus thickness: painful DSP insensate vs. HV (P = 0.004), no DSP (P = 0.003), painless DSP (P = 0.05), and painful DSP sensate (P = 0.002).

Downloaded from http://diabetesjournals.org/diabetes/article-pdf/68/4/796/523542/db180509.pdf by guest on 27 August 2022

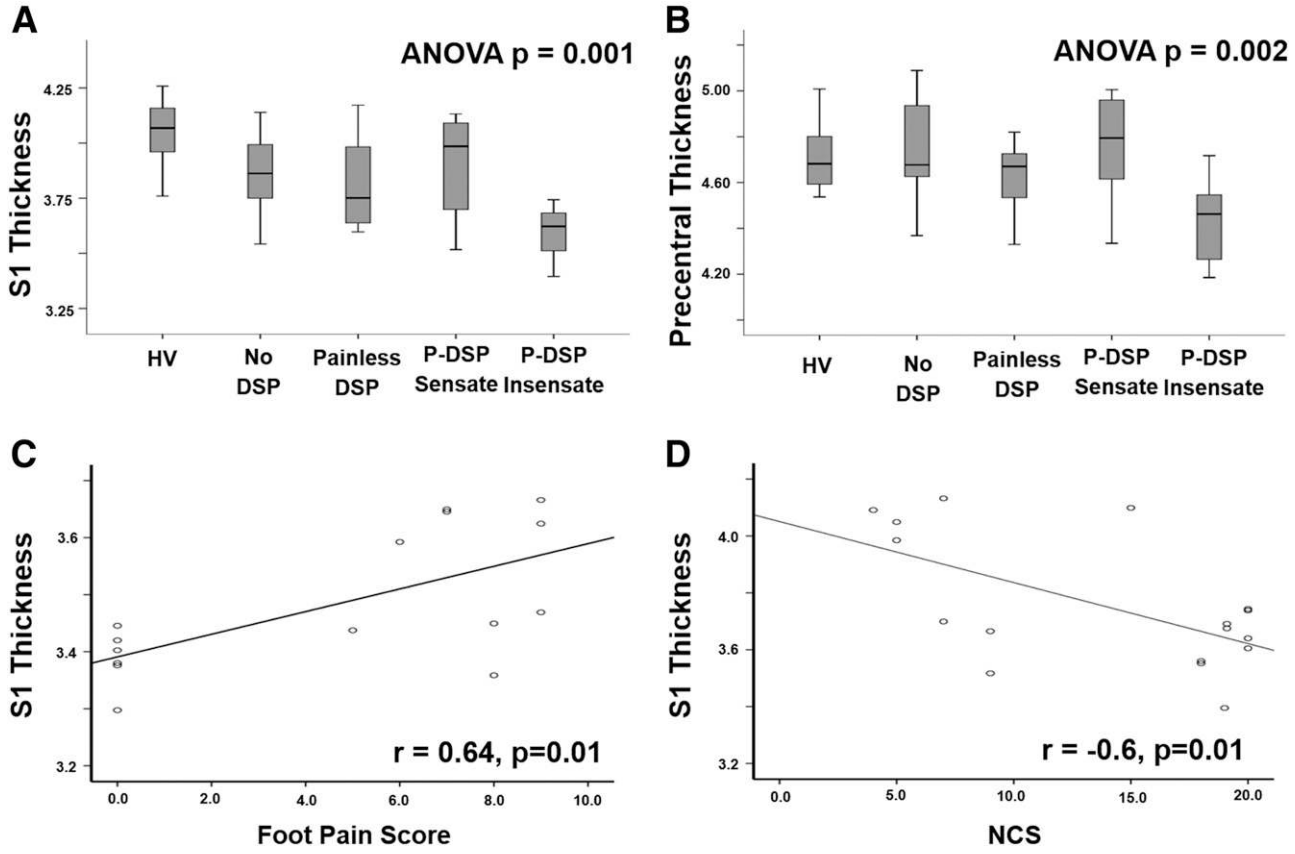

Figure 2—*A* and *B*: Box-and-whisker plots (median and quartiles) of postcentral gyrus and precentral gyrus cortical thickness (in mm) for each study cohort. *C* and *D*: Spearman rank correlation between S1 cortical thickness (in mm) and foot pain score and NCS S1 cortical thickness for subjects with painful (P) DSP sensate and P-DSP insensate.

a significant relationship between the activation intensity in the face/lip region and severity of neuropathy (NCS $r = 0.74$, $P < 0.001$), neuropathic pain score (NTSS-6 $r = -0.45$, $P = 0.04$), evoked foot pain score ($r = -0.46$, $P = 0.03$), and S1 cortical thickness ($r = -0.57$, $P = 0.01$) (Supplementary Fig. 4).

DISCUSSION

Using a multimodal neuroimaging approach, these data show a reduction in S1 cortical thickness and a remapping of S1 sensory processing in patients with painful DSP insensate and that the magnitude of cortical response in the face/lip S1 region to tonic heat stimulation is negatively correlated with S1 cortical thickness. Furthermore, the extent to which S1 structure and function is altered is related to the severity of neuropathy and the magnitude of self-reported and tonic heat-evoked pain intensity ratings. Thus, only in the painful DSP insensate group is the altered structural and functional organization of S1 linked to both behavioral and brain responses to heat hyperalgesia. This study is the first in our knowledge to demonstrate a relationship between patient sensory phenotypes and brain structural and functional changes in DSP.

Although the painful/painless diabetic foot has long been recognized, there has been a lack of a pathophysiological explanation for such patients who have severe neuropathic pain in the absence of sensation in their feet (40). Advances have been made in the sensory profiling of patients with diabetes (Pain in Neuropathy Study [PiNS]) (4) as well as early indications that an individual's pain phenotype may predict response to treatment (41). However, a pathophysiological explanation at both the peripheral and the central level for these phenotypes is limited. The current study has tried to explore in carefully phenotyped patients whether a correlation exists between CNS structural/functional changes and various sensory phenotypes. Patients with painful DSP insensate had the greatest severity of neuropathy (NCS) and the greatest reduction in S1 cortical thickness. Hence, the most likely explanation for the reduction in S1 cortical thickness is deafferentation or a dying-back axonopathy that principally affects the sensory neurons in DSP. This explanation is in keeping with our previous findings (5,15,16,42,43), but we also demonstrate a widening of S1 functional representation of both the foot and the thigh in patients with painful DSP insensate. It is plausible that the reduction in cortical thickness has led to recruitment of viable/functioning

Downloaded from http://diabetesjournals.org/diabetes/article-pdf/68/4/796/523542/db180509.pdf by guest on 27 August 2022

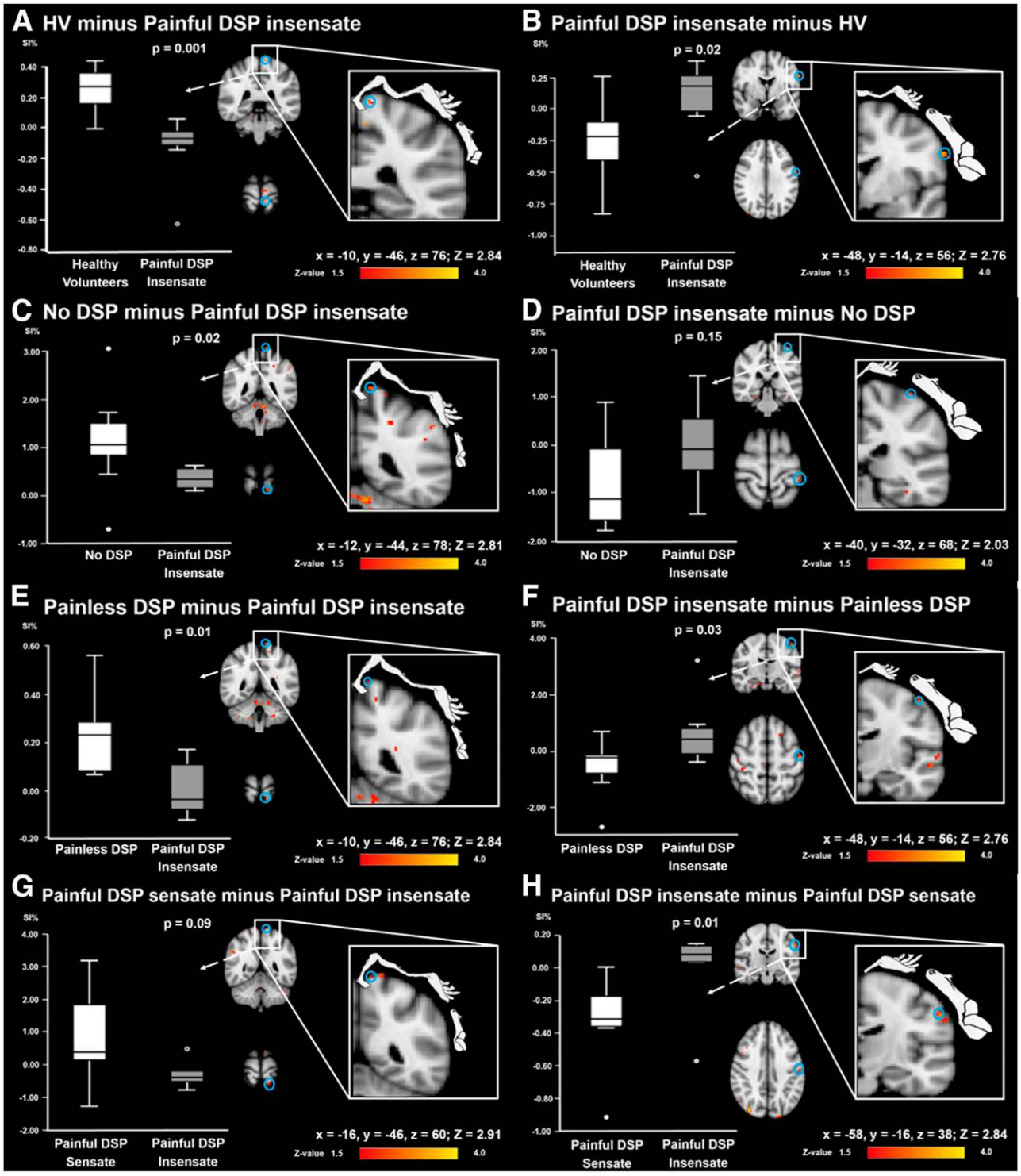

Figure 3—Whole-brain voxel-wise group analysis of tonic heat stimulation of the foot for subjects with painful DSP insensate compared with HVs (*A* and *B*) and subjects with no DSP (*C* and *D*), painless DSP (*E* and *F*), and painful DSP sensate (*G* and *H*). The map shows activation that exceeds a threshold of $Z > 1.5$ and a family-wise error–corrected cluster significance threshold of $P < 0.05$ (for display only). *A*, *C*, *E*, and *G*: The blue circle demonstrates the region of greatest activation within the S1 in HVs and subjects with no DSP, painless DSP, and painful DSP sensate compared with subjects with painful DSP insensate. *B*, *D*, *F*, and *H*: The blue circle demonstrates the region of greatest activation within the S1 in subjects with painful DSP insensate compared with the other study cohorts. Box plots display median, interquartile range, and minimum and maximum values for percent change in signal intensity (SI%) from the region of greatest activation highlighted by the blue circle. Subjects with painful DSP insensate showed displacement of the lateral border of the foot into the face/lip area. Group comparisons of parameter estimates were performed using Mann-Whitney *U* test, and $P < 0.05$ (two-tailed) indicated significance.

Downloaded from http://diabetesjournals.org/diabetes/article-pdf/68/4/796/523542/db180509.pdf by guest on 27 August 2022

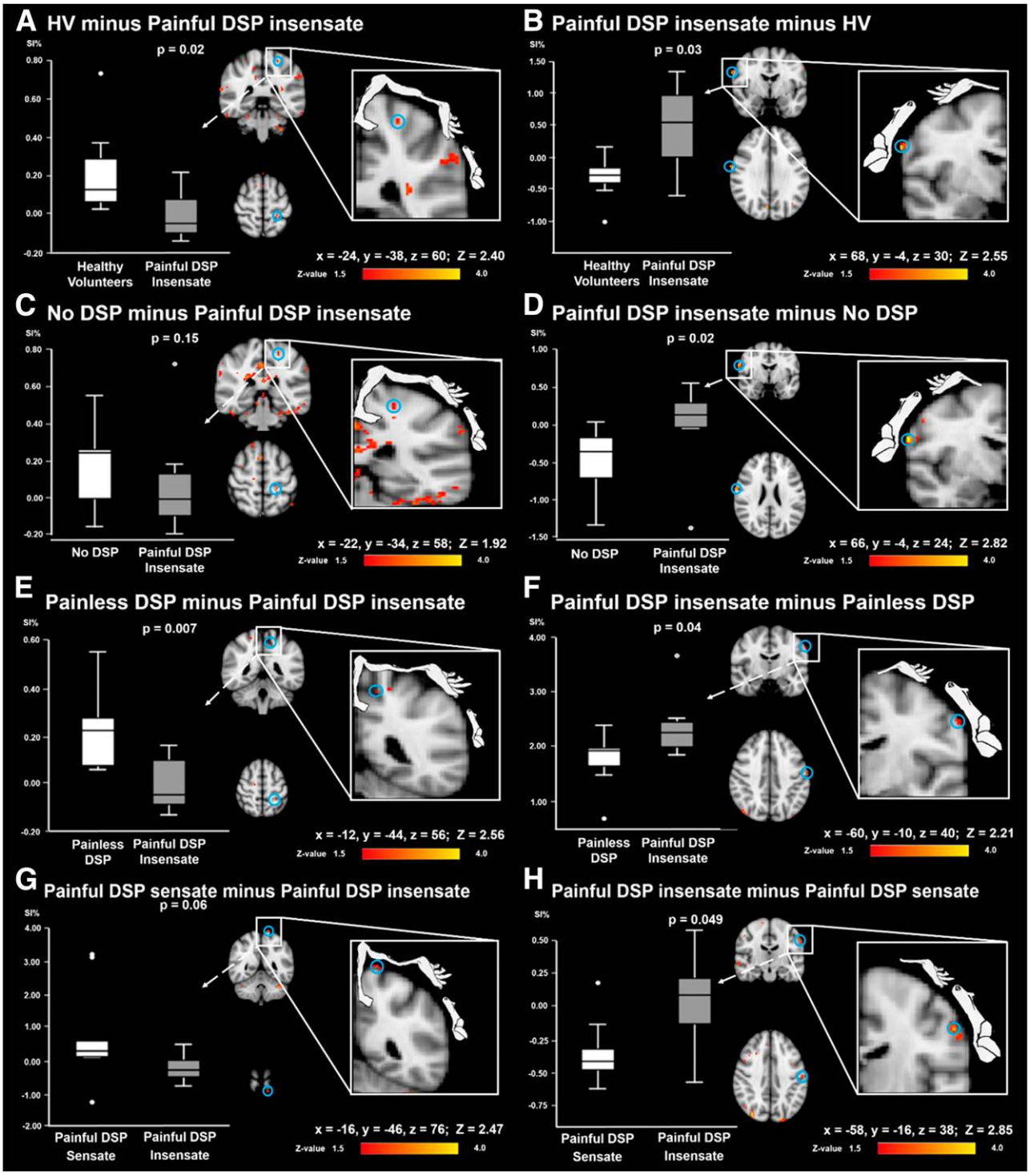

Figure 4—Within-group analysis of tonic heat stimulation of the thigh for subjects with painful DSP insensate compared with HVs (*A* and *B*) and subjects with no DSP (*C* and *D*), painless DSP (*E* and *F*), and painful DSP sensate (*G* and *H*). *A*, *C*, *E*, and *G*: The blue circle demonstrates the region of greatest activation within the S1 in HVs and subjects with no DSP, painless DSP, and painful DSP sensate compared with subjects with painful DSP insensate. *B*, *D*, *F*, and *H*: The blue circle demonstrates the region of greatest activation within the S1 in subjects with painful insensate compared with the other study cohorts. Box plots display median, interquartile range, and minimum and maximum values for percent change in signal intensity (SI%) from the region of greatest activation highlighted by the blue circle. Subjects with painful DSP insensate showed displacement of the lateral border of the thigh into the face/lip area. Group comparisons of parameter estimates were performed using Mann-Whitney *U* test, and $P < 0.05$ (two-tailed) indicated significance.

Downloaded from http://diabetesjournals.org/diabetes/article-pdf/68/4/796/523542/db180509.pdf by guest on 27 August 2022

neurons in adjacent areas, which is similar to findings reported in previous studies of amputees with phantom limb pain (44). Of note, there was a negative relationship between the magnitude of cortical response in the face/lip region to tonic heat stimulation with S1 cortical thickness and both evoked pain and chronic neuropathic pain severity, suggesting that reduction in cortical thickness results in fewer viable neurons and less overall pain perception. In addition, further studies should examine the role of pain as a cause and/or consequence of the CNS changes described. Another possible explanation that needs future exploration is the impact of diabetes status on these findings. S1 cortical thickness was lower in the diabetes groups compared with HVs, which would suggest that diabetes also affects the brain structural changes described. Finally, although our findings suggest that the changes in S1 structural and functional organization is driven by the neuropathic process, other pain-related behavioral changes, such as physical functioning, deprivation of social contacts, and mood, also may contribute to brain neuroplasticity. Our study was not designed to explore the interaction of these various factors on brain changes in chronic pain. Furthermore, prospective studies in well-characterized patients will be required to examine this.

This study is limited by its relatively small sample size; however, the subjects were well characterized, and we believe that the study provides a novel insight into the CNS neural correlates of various clinical pain phenotypes in DSP. The results obtained are robust ($P < 0.05$), even after correction for multiple comparisons using the family-wise error method. In addition, we examined only subjects with type 1 diabetes. Although the pathophysiology of nerve injury in type 2 diabetes may be different, we postulate similar alterations within the CNS. Nevertheless, further studies in subjects with type 2 diabetes are warranted. There was also a significant difference in sex distribution across study cohorts, but this is unlikely to have a significant impact on the assessments because MRI images were registered to a standard space that removes global differences in cortical morphometry that may be related to sex, hemispheric asymmetries, or age. Furthermore, no significant differences were found between males and females in the psychophysical responses to nociceptive stimulation to the foot and thigh (temperature, pain, and unpleasantness scores). Hence, subgroup differences in sex distribution is unlikely to affect the functional activation of the somatosensory cortex. Finally, apart from the HV cohort, there was a male preponderance in all the other (diabetes) subgroups, including the disease control group comprising subjects with diabetes and no DSP. No statistically significant differences were present between control groups (HV vs. no DSP). Nevertheless, important sex differences exist in the prevalence of painful diabetic neuropathy and other chronic pain conditions. A larger study with a different design is required to truly examine sex differences in functional organization of the S1. Several critical lines of future work have emerged from this study, including longitudinal prospective studies to determine the natural history of brain structural and functional changes in DSP and to truly dissect whether and how these are causally related.

Acknowledgments. The authors acknowledge the hard work, skills, and contributions of the radiographers at the Academic Unit of Radiology. The authors also greatly appreciate the study volunteers who spent considerable time participating in this study.

Funding. This study was funded by a grant from JDRF International (1-2008-69).

Duality of Interest. No potential conflicts of interest relevant to this article were reported.

Author Contributions. D.S. recruited participants, undertook clinical and neurophysiological assessments, researched and analyzed clinical and MR data, and wrote the manuscript. I.D.W. undertook planning of MR experiments and reviewed and revised the manuscript. F.F. analyzed MR cortical thickness data. A.S., J.D., and E.B. undertook clinical and neurophysiological assessments and assisted with participant recruitment. J.H. undertook clinical and neurophysiological assessments, assisted with participant recruitment, and assisted with analyzing MR data. G.R. supervised neurophysiological assessments and reviewed and revised the manuscript. R.G. reviewed and revised the manuscript. I.T. supervised MRI experiments, assisted with data analysis and interpretation, and reviewed and revised the manuscript. S.T. supervised the project and reviewed and revised the manuscript. S.T. is the guarantor of this work and, as such, had full access to all the data in the study and takes responsibility for the integrity of the data and the accuracy of the data analysis.

Data Availability. The data sets generated and/or analyzed during the study are available from the corresponding author upon reasonable request.

References

1. Dyck PJ, Kratz KM, Karnes JL, et al. The prevalence by staged severity of various types of diabetic neuropathy, retinopathy, and nephropathy in a population-based cohort: the Rochester diabetic neuropathy study. Neurology 1993;43:817–824

2. Tesfaye S, Boulton AJ, Dickenson AH. Mechanisms and management of diabetic painful distal symmetrical polyneuropathy. Diabetes Care 2013;36:2456–2465

3. Feldman EL, Nave KA, Jensen TS, Bennett DLH. New horizons in diabetic neuropathy: mechanisms, bioenergetics, and pain. Neuron 2017;93:1296–1313

4. Themistocleous AC, Ramirez JD, Shillo PR, et al. The Pain in Neuropathy Study (PiNS): a cross-sectional observational study determining the somatosensory phenotype of painful and painless diabetic neuropathy. Pain 2016;157:1132–1145

5. Selvarajah D, Wilkinson ID, Davies J, Gandhi R, Tesfaye S. Central nervous system involvement in diabetic neuropathy. Curr Diab Rep 2011;11:310–322

6. Marshall AG, Lee-Kubli C, Azmi S, et al. Spinal disinhibition in experimental and clinical painful diabetic neuropathy. Diabetes 2017;66:1380–1390

7. Segerdahl AR, Themistocleous AC, Fido D, Bennett DL, Tracey I. A brain-based pain facilitation mechanism contributes to painful diabetic polyneuropathy. Brain 2018;141:357–364

8. Lee MC, Tracey I. Imaging pain: a potent means for investigating pain mechanisms in patients. Br J Anaesth 2013;111:64–72

9. Merzenich MM, Nelson RJ, Stryker MP, Cynader MS, Schoppmann A, Zook JM. Somatosensory cortical map changes following digit amputation in adult monkeys. J Comp Neurol 1984;224:591–605

10. Birbaumer N, Lutzenberger W, Montoya P, et al. Effects of regional anesthesia on phantom limb pain are mirrored in changes in cortical reorganization. J Neurosci 1997;17:5503–5508

11. Flor H, Elbert T, Knecht S, et al. Phantom-limb pain as a perceptual correlate of cortical reorganization following arm amputation. Nature 1995;375:482–484

Downloaded from http://diabetesjournals.org/diabetes/article-pdf/68/4/796/523542/db180509.pdf by guest on 27 August 2022

12. Wrigley PJ, Press SR, Gustin SM, et al. Neuropathic pain and primary somatosensory cortex reorganization following spinal cord injury. Pain 2009;141:52–59
13. Lotze M, Flor H, Grodd W, Larbig W, Birbaumer N. Phantom movements and pain. An fMRI study in upper limb amputees. Brain 2001;124:2268–2277
14. Eaton SE, Harris ND, Rajbhandari SM, et al. Spinal-cord involvement in diabetic peripheral neuropathy. Lancet 2001;358:35–36
15. Selvarajah D, Wilkinson ID, Emery CJ, et al. Early involvement of the spinal cord in diabetic peripheral neuropathy. Diabetes Care 2006;29:2664–2669
16. Selvarajah D, Wilkinson ID, Maxwell M, et al. Magnetic resonance neuroimaging study of brain structural differences in diabetic peripheral neuropathy. Diabetes Care 2014;37:1681–1688
17. Apkarian AV, Sosa Y, Sonty S, et al. Chronic back pain is associated with decreased prefrontal and thalamic gray matter density. J Neurosci 2004;24:10410–10415
18. Schaechter JD, Moore CI, Connell BD, Rosen BR, Dijkhuizen RM. Structural and functional plasticity in the somatosensory cortex of chronic stroke patients. Brain 2006;129:2722–2733
19. DaSilva AF, Becerra L, Pendse G, Chizh B, Tully S, Borsook D. Colocalized structural and functional changes in the cortex of patients with trigeminal neuropathic pain. PLoS One 2008;3:e3396.
20. Bril V. NIS-LL: the primary measurement scale for clinical trial endpoints in diabetic peripheral neuropathy. Eur Neurol 1999;41(Suppl. 1):8–13
21. Dyck PJ, O'Brien PC, Kosanke JL, Gillen DA, Karnes JLA. A 4, 2, and 1 stepping algorithm for quick and accurate estimation of cutaneous sensation threshold. Neurology 1993;43:1508–1512
22. Dyck PJ, Zimmerman I, Gillen DA, Johnson D, Karnes JL, O'Brien PC. Cool, warm, and heat-pain detection thresholds: testing methods and inferences about anatomic distribution of receptors. Neurology 1993;43:1500–1508
23. Pfeifer M. Cardiovascular assessment. In *Diabetic Neuropathy*. 2nd ed. Dyck PJ, Thomas PK, Eds. Philadelphia, Saunders, 1999, p. 171–183
24. Dyck PJ, Davies JL, Litchy WJ, O'Brien PC. Longitudinal assessment of diabetic polyneuropathy using a composite score in the Rochester Diabetic Neuropathy study cohort. Neurology 1997;49:229–239
25. Finnerup NB, Haroutounian S, Kamerman P, et al. Neuropathic pain: an updated grading system for research and clinical practice. Pain 2016;157:1599–1606
26. Bastyr EJ III, Price KL, Bril V; MBBQ Study Group. Development and validity testing of the neuropathy total symptom score-6: questionnaire for the study of sensory symptoms of diabetic peripheral neuropathy. Clin Ther 2005;27:1278–1294
27. Maier C, Baron R, Tölle TR, et al. Quantitative sensory testing in the German Research Network on Neuropathic Pain (DFNS): somatosensory abnormalities in 1236 patients with different neuropathic pain syndromes. Pain 2010;150:439–450
28. Tesfaye S, Boulton AJ, Dyck PJ, et al.; Toronto Diabetic Neuropathy Expert Group. Diabetic neuropathies: update on definitions, diagnostic criteria, estimation of severity, and treatments [published correction appears in Diabetes Care 2010;33:2725]. Diabetes Care 2010;33:2285–2293
29. Atlas LY, Bolger N, Lindquist MA, Wager TD. Brain mediators of predictive cue effects on perceived pain. J Neurosci 2010;30:12964–12977
30. Reuter M, Rosas HD, Fischl B. Highly accurate inverse consistent registration: a robust approach. Neuroimage 2010;53:1181–1196
31. Ségonne F, Dale AM, Busa E, et al. A hybrid approach to the skull stripping problem in MRI. Neuroimage 2004;22:1060–1075
32. Fischl B, Salat DH, Busa E, et al. Whole brain segmentation: automated labeling of neuroanatomical structures in the human brain. Neuron 2002;33:341–355
33. Fischl B, Salat DH, van der Kouwe AJ, et al. Sequence-independent segmentation of magnetic resonance images. Neuroimage 2004;23(Suppl. 1):S69–S84
34. Fischl B, Liu A, Dale AM. Automated manifold surgery: constructing geometrically accurate and topologically correct models of the human cerebral cortex. IEEE Trans Med Imaging 2001;20:70–80
35. Ségonne F, Pacheco J, Fischl B. Geometrically accurate topology-correction of cortical surfaces using nonseparating loops. IEEE Trans Med Imaging 2007;26:518–529
36. Dale AM, Fischl B, Sereno MI. Cortical surface-based analysis. I. Segmentation and surface reconstruction. Neuroimage 1999;9:179–194
37. Fischl B, Dale AM. Measuring the thickness of the human cerebral cortex from magnetic resonance images. Proc Natl Acad Sci U S A 2000;97:11050–11055
38. Smith SM, Jenkinson M, Woolrich MW, et al. Advances in functional and structural MR image analysis and implementation as FSL. Neuroimage 2004;23(Suppl. 1):S208–S219
39. Winkler AM, Ridgway GR, Webster MA, Smith SM, Nichols TE. Permutation inference for the general linear model. Neuroimage 2014;92:381–397
40. Veves A, Manes C, Murray HJ, Young MJ, Boulton AJ. Painful neuropathy and foot ulceration in diabetic patients. Diabetes Care 1993;16:1187–1189
41. Demant DT, Lund K, Vollert J, et al. The effect of oxcarbazepine in peripheral neuropathic pain depends on pain phenotype: a randomised, double-blind, placebo-controlled phenotype-stratified study. Pain 2014;155:2263–2273
42. Selvarajah D, Wilkinson ID, Emery CJ, et al. Thalamic neuronal dysfunction and chronic sensorimotor distal symmetrical polyneuropathy in patients with type 1 diabetes mellitus. Diabetologia 2008;51:2088–2092
43. Selvarajah D, Wilkinson ID, Gandhi R, Griffiths PD, Tesfaye S. Microvascular perfusion abnormalities of the thalamus in painful but not painless diabetic polyneuropathy: a clue to the pathogenesis of pain in type 1 diabetes. Diabetes Care 2011b;34:718–720
44. Kew JJ, Ridding MC, Rothwell JC, et al. Reorganization of cortical blood flow and transcranial magnetic stimulation maps in human subjects after upper limb amputation. J Neurophysiol 1994;72:2517–2524

Downloaded from http://diabetesjournals.org/diabetes/article-pdf/68/4/796/523542/db180509.pdf by guest on 27 August 2022